CEBAF-PR-92-022
CLAS-NOTE 92-012

Characteristics of Yerevan High Transparency Scintillators

M.Amaryan, G.Asryan, R.Demirchyan, K.Egiyan, Yu.Sharabyan, S.Stepanyan, M.Tarverdyan
Yerevan Physics Institute, Yerevan, Armenia

V.Burkert, C.Zorn
CEBAF, Newport News, Virginia, USA

Abstract

Optical transmission, light output and time characteristics are given for long scintillator strips fabricated at the Yerevan Physics Institute using the extrusion method. It is shown that at 45% relative (to anthracene) light output, good transmission (2.5÷2.9 m attenuation length with photomultiplier direct readout and 3÷3.5 m attenuation length fiber readout) and time characteristics (average decay time 2.8 nsec) were obtained.

1. Introduction.

In modern large acceptance detectors very long plastic scintillators (PS) are needed. For example, in the Time-of-Flight and Electromagnetic Shower Calorimeter systems of the CEBAF CLAS detector up to 4.6m long PS will be used. In the one of the SSC detector more then 10m long PS are proposed.

For uniform amplitude and time resolution these scintillators should have high transparency and reasonable light output. Fabrication of PS with such characteristics using traditional methods (polymerization-mechanical processing-polishing) is difficult and expensive.

There are several centers around the world with significant success in producing of long PS with high transparency: Bicron (USA)/1/; NE-Technology (UK)/2/; Kuraray (Japan)/3/. The technology used by these companies is on an industrial scale and requires large and expensive installations, such as large size ovens and milling modules. On the other hand the much simpler extrusion method can be employed by small institutions

or even by small groups. This method allows fabrication /4/ of long scintillators with **the complicated cross section profile.** The main disadvantage of this method is the limitation in scintillator thickness ($\leq$20mm) and widths ($\leq$200mm).

During the past twenty five years, techniques for the production of high quality scintillator material were developed at the Yerevan Physics Institute. Recently, a facility for the extrusion of long scintillator was constructed. In this report the main physical and optical characteristics of the first batch of long scintillator bars produced at Yerevan are reported.

2. The Extruder.

The extrusion facility (Extruder) consists of two main parts (Fig.1).

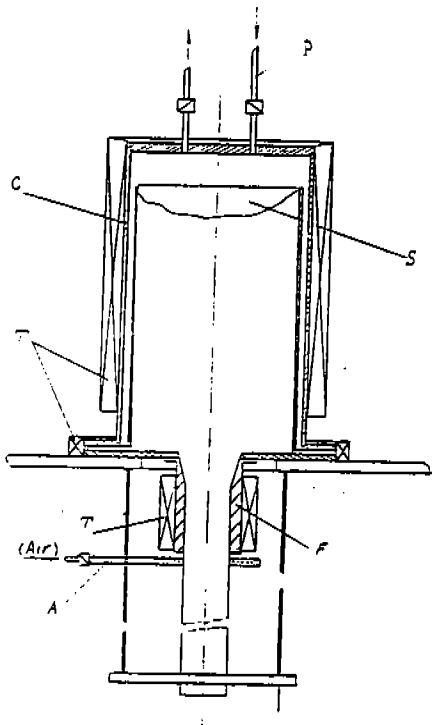

Fig.1 *Schematic Plane of Extruder: C - Cylindrical Hermetical Container; S - Plastic Scintillator; F - Filiera; T - Heating System; A - Air Cooling; P - Inert Gas Pressure.*

A cylindrical hermetical container (CHC) 300mm in diameter and 700mm in height, and a scintillator forming device, called Filiera, which is attached to the CHC. Both parts of the extruder are equipped with a heating systems for generating temperatures in the

inner volume of the extruder of up to 200°(C) with a stability of 0.5°.

The scintillator material in the form of a cylinder 295mm in diameter and 500mm in height was placed in the CHC. At a temperature of 150÷170° in the CHC, pressure was applied to the CHC using inert gas at 4÷8 atm. The temperature of the Filiera was 120÷ 140°. Air cooling was used at the exit of the Filiera for fixing the scintillator profile. Calibrated rubber compensators and a weight of 100÷200gr was applied to provide constant tension. The required tolerances of scintillator's width and thickness were achieved by choosing and permanently controlling of extrusion rate. For this the variations of all three parameters: temperature, applied weight and gas pressure were used. The typical extrusion velocity for 10×100 mm^2 cross section scintillator was 1.5 cm/min.

3. Scintillators characteristics.

3.1. The **spectral (transmission and fluorescence) characteristics** of the scintillator material(SM) was studied by the Fermilab Detector Group.

In Fig.2 a typical transmission spectrum of SM (the cylindrical form sample 2cm in diameter and 2cm in height) is shown.

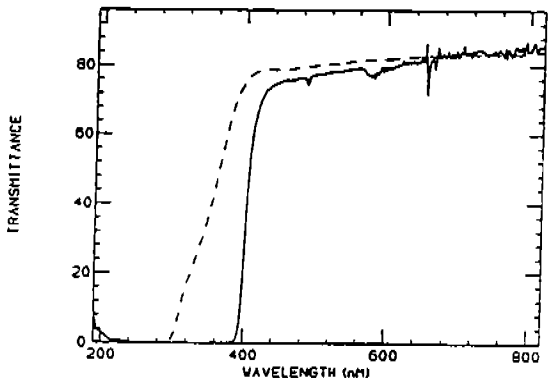

Fig.2 *Transmission characteristics of scintillator material (solid curve) and of polystyrene (dashed curve).*

One can see that this SM is transparent in the wavelength region above 400 nm.

In Fig.3a the fluorescence emission spectrum of the same sample is presented. It was measured by illuminating the scintillator with UV light of λ= 254nm. The polystyrene base material was excited and its emission spectrum was shifted by two wavelength shifters: p-terphenyl + 4^4 Distyryl Biphenol. This spectrum is cut at the left side due to absorption in the plastic (see Fig.2) and self-absorption of the shifters . This effect is illustrated in Fig.3b. The so called front-face fluorescence emission spectrum is obtained when the scintillator is illuminated by UV light of λ=313nm at an incident angle of 45^0 and when the surface emission is viewed at 90^0 to the incident light direction. In this case the first w-shifter (p-terphenyl) is excited and the two peaks are the emission spectra of the two

shifters (p-terphenyl left peak, 4^4 Distyryl Biphenol - right one).

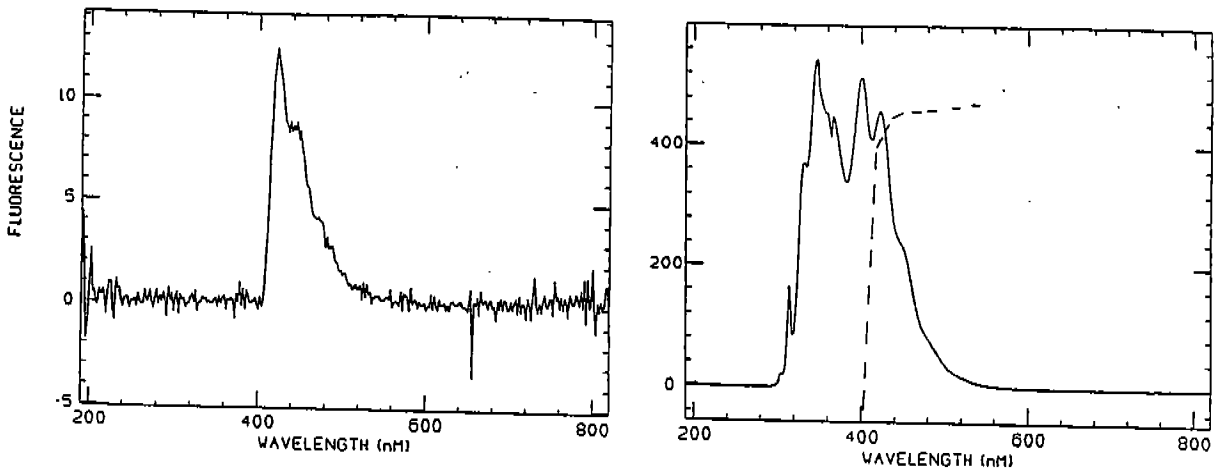

Fig.3: *a)- Fluorescence emission spectrum upon illumination of the scintillator with UV light of λ=254nm. b)- Front-face emission spectrum at illumination of the scintillator with UV light of 313nm. The p-terphenyl (left) and 4^4 Distyryl Biphenol (right) peaks are seen.*

The dashed line indicates the plastic's transparency region (see Fig.2).

A significant part of the final spectrum (the region $\lambda \leq$400nm) will be lost due to the absorption in the plastic, which results in a reduction of the light output (see below). For having more light output a second w-shifter with larger Stokes shift should be used. On the other hand the larger the wavelength of the second w-shifter the larger the scintillator's decay time /1/

3.2 The **light output** of the scintillators was measured in two cases.

In the first case the scintillator material was tested. Two samples of PS and anthracene of similar shape were irradiated by a ^{60}Co radioactive source ($\approx$ 1 MeV γ pack and a β spectrum with maximum energy 0.318MeV) and were viewed by the same PMT. The light output was estimated using the photopeak positions. A 45% relative light output to the anthracene was obtained.

In the second case the light output of extruded scintillator strips of 2m length and 1×10 cm^2 cross section was measured.

These measurements were performed at CEBAF. The experimental setup and block scheme of the electronics are shown in fig.4 /5/.

The scintillator bar, two XP2262 type PMTs and a radioactive PMTs (PMT1) source (^{207}Bi with 1 MeV electron line) were housed in a 6m long light-tight box. One of these PMTs was used to measure the light from one end of the scintillator. It was optically coupled to the scintillator via BC-630 silicone optical grease. The second PMT (PMT2) was used for triggering and was located on the opposite side of the scintillator with its photocathode facing the radioactive source /5/. The distance of the PMT2 photocathode and the scintillator surface was 10mm. The PMT2 and the radioactive source were mounted

on a cart that could be moved along the scintillator by a computer controlled motor drive. CERN-made bases and commercial electronics units (Discriminators, Logic Units, TDC, ADC) were used.

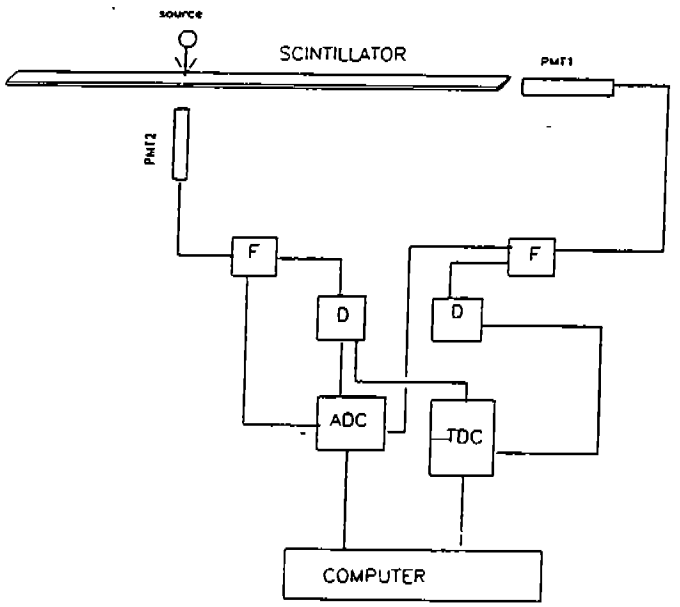

Fig.4: *Test setup. F - Fan out; D - Discriminators.*

The light output of the long scintillators was measured by determining the average number of photoelectrons from the PMT1 photocathode at 1 MeV energy deposit in the scintillator. The 1 MeV line was selected by PMT2.

In Fig.5 the ADC spectrum of PMT2 is presented. The right side peak corresponds to the 1 MeV electron line. For triggering only events under this peak were used.

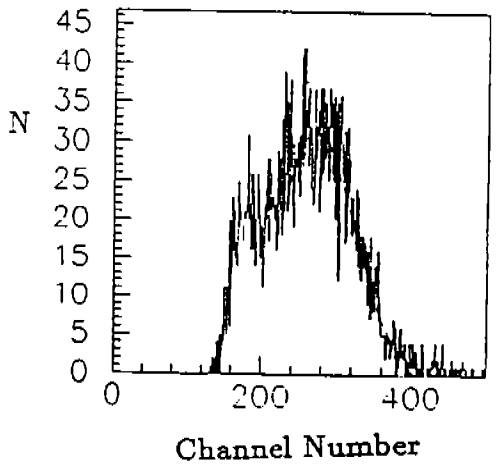

Fig.5 *ADC spectrum of PMT2. Right sid peak coresponds to 1MeV (^{207}Bi) energy deposit and is fitted to Gaussian distribution.*

The average number of photoelectrons was obtained by measuring the pulse height distribution of PMT1 in two regimes. In the first case, the full scintillation light flux was detected while in second case the light flux to the PMT1 photocathode was reduced (using the natural filter) to the one photoelectron registration regime.

In Fig.6 these two ADC distributions are shown.

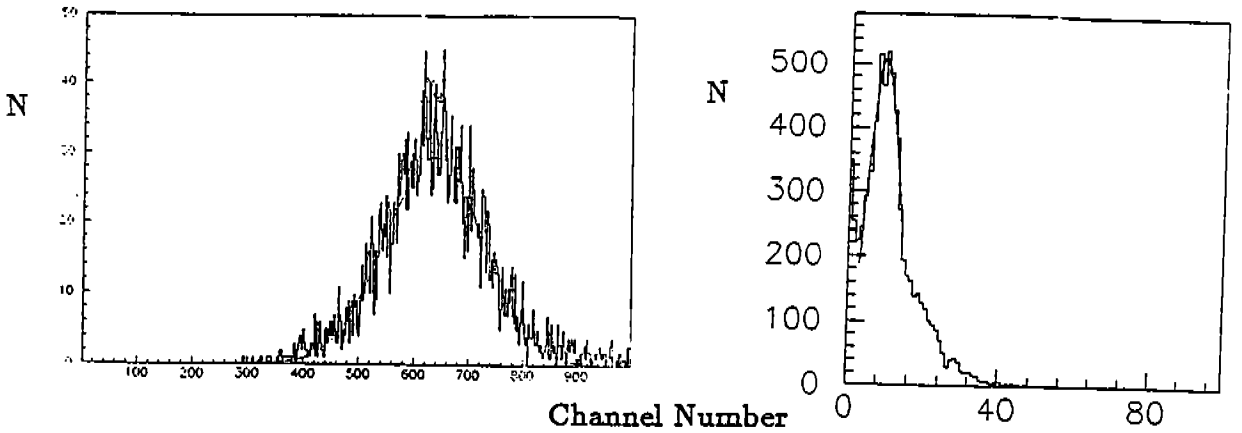

Fig.6 *ADC spectra of PMT1 with Gaussin fits: a)-full scintillation light detection; b)- single photoelectron registration regime.*

The average number of photoelectrons is proportional to the ratio of mean values of these two distributions if the differences (a_0) of mean values of the i and $i-1$ photoelectron's distributions are equal to the centroid of single photoelectron distribution (a_1). However, since the location of the pedestal in ADC channel scale does not corresponds just to the "0" photoelectrons the a_0 can differ from the a_1.

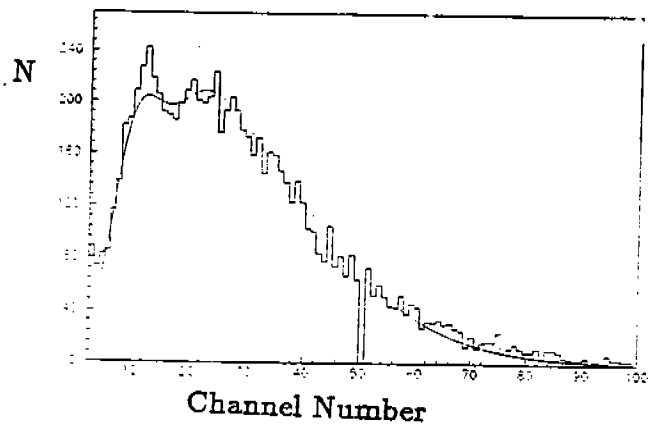

Fig.7 *ADC spectrum of PMT1 in the few photoelectron registration regime, fitted by (1)÷(3) (see text).*

For estimation of a_0 the light flux to the PMT1 photocathode was increased to 3-4 photoelectrons. The spectrum in the 1÷4 photoelectron region is shown in Fig.7. Gauss distributions for all one, two, three, four photoelectron contributions and Poisson distributions for their weights were assumed. The spectrum in Fig.7 was therefore fitted using the form

$$A = C \cdot \sum P_i(n_{pe}) \cdot C_i(n_{ch}) \qquad (1)$$

where

$$P_i(n_{pe}) = \frac{n_{pe}^i \cdot e^{-n_{pe}}}{i!} \tag{2}$$

and

$$C_i(n_{ch}) = \frac{1}{\sigma_1 \cdot \sqrt{i}} \cdot e^{-(\frac{n_{ch} - (a_1 + (i-1) \cdot a_0)}{2 \cdot \sigma_1 \cdot \sqrt{i}})^2} \tag{3}$$

In (1)÷(3) n_{pe} is the average number of photoelectrons, n_{ch} is the current number of the ADC channels, i is the number of photoelectrons, a_1 and σ_1 are the mean value and the standard deviation of the Gauss distribution of the single photoelectrons, respectively, $a_1 + (i-1) \cdot a_0$ and $\sigma_1 \cdot \sqrt{i}$ are the corresponding values for "i" number of photoelectrons, respectively. The fit to the spectrum in Fig.10 using (1)÷(3) with free parameter a_0 yields a value $a_0 = 0.95 \cdot a_1$.

Thus, the average number of photoelectrons released from the photocathode of PMT1 can be defined as

$$n_{pe} = \frac{\Delta s}{s} \cdot (\frac{A_a - a_1}{a_0} + 1) \tag{4}$$

where A_a is the mean value of the Gaussian fit to the spectrum in Fig.6a, s and Δs are the scintillator cross section and its fraction covered by PMT1, respectively. Since the thickness of the scintillator strips is 10 mm and the diameter of PMT1 photocathode is 44 mm, $\frac{\Delta s}{s} = 0.44$. Taking A_a from Fig.6a and a_1 from Fig.6b we find

$$n_{pe}^Y \approx 150/MeV$$

The same measurements using BC-412 scintillators yields

$$n_{pe}^B \approx 200/MeV$$

i.e. the light output of the Yerevan scintillator is $\approx 75\%$ of of the BC-412 scintillator. Since the light output of BC-412 scintillator is 60% to anthracene we conclude that the light output of Yerevan strips is 45% of anthracene in accordance with the previous results. Hence, the light output of SM does not decrease in the extrusion process.

3.3 The decay time of the scintillators was investigated using the 1 MeV electron line of ^{207}Bi (see above). The decay time was obtained by measuring the time difference between the anode signals of PMT1 and PMT2 in the single photoelectron regime of PMT1 (see above). In Fig.9 a typical TDC spectrum of the decay time is presented which was

obtained by irradiating the scintillator at a 10 cm distance from PMT1. The right side of this spectrum is fitted by an exponential distribution

$$T = T_0 \cdot \exp^{-t/\tau_0} \tag{5}$$

where

$$\tau_0^Y = (2.8 \pm 0.21) ns$$

is the scintillation average decay time.

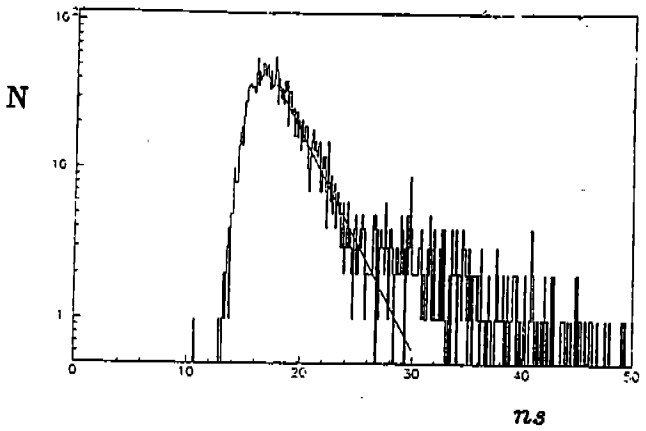

Fig.8 *TDC spectrum (decay time) for single photoelectron registration by PMT1. The right side is fitted to the exponentiol function (5).*

The same measurements for BC-412 yield

$$\tau_0^B = (3.6 \pm 0.25) ns$$

3.4 The **attenuation characteristics** are most important for long scintillators. For studying these characteristics the experimental setup was slightly modified. Instead of PMT2 (and r.a. source) a continuous (8 KeV, 60 w.) X-ray source was used /6/, and the DC anode current of the PMT1 as a function of the distance to the PMT1 was measured. In all measurements the dark current of the PMT1 was measured and was found to be no more than 3% of the minimal value of measured current. This value was subtracted from the measured current. Fig.9a shows some results typical. The measured data were fitted to a double exponential dependence

$$A = P_1 \cdot \exp^{-x/P_2} + P_3 \cdot \exp^{-x/P_4} \tag{6}$$

Tables 1÷3 summarize the fit results of measurements with direct readout.

Table 1 include data obtained with blacked away side end of scintillator. The results for the BC-412 and SCSN81 type scintillators are presented for comparison. One can see that the attenuation length the Yerevan scintillators are similar to those of BC-412 and SCSN81 scintillators.

Table 1.

Scintillator	P_4	P_2	P_1/P_3	χ^2/NDF
YER - 2	250±0.5	16.3±0.05	0.63±0.009	1.51
YER - 3	230±0.5	18.6±0.02	0.52±0.004	6.23
YER - 5	274±2.1	17.2±0.11	0.62±0.004	3.66
YER - 7	240±0.5	15.6±0.05	0.58±0.004	4.88
BC-412	275±1	16.1±0.07	0.25±0.015	9.0
SCSN81	271±4.	45±0.5	0.30±0.01	4.5

Table 2 and 3 shows the attenuation characteristics of Yerevan scintillators when second end was open and/or covered by reflector.

Table 2.

Scintillator	P_4	P_2	P_1/P_3	χ^2/NDF
YER - 2	329±0.9	19.5±0.03	0.65±0.009	4.01
YER - 3	290±1.6	22.9±0.07	0.57±0.004	10.1
YER - 5	348±2.1	19.4±0.11	0.68±0.004	4.92
YER - 7	316±0.9	23.3±0.03	0.65±0.004	6.53

Table 3.

Scintillator	P_4	P_2	P_1/P_3	χ^2/NDF
YER - 2	686±2.2	20±0.33	0.61±0.009	7.20
YER - 3	613±5.2	23.5±0.04	0.62±0.004	10.3
YER - 5	1090±48	23.6±0.54	0.54±0.004	5.91
YER - 7	661±45	23.5±0.02	0.56±0.004	7.18

All of the above data were obtained when PMT1 was directly coupled to the right end of the scintillators. Recently, a new Fiber Optic (FO) readout system was developed /6/ for use discussed type scintillators.

Table 4.

Scintillator	P_4	P_2	P_1/P_3	χ^2/NDF
YER - 2	314±1.0	24.0±0.1	0.43±0.010	1.21
YER - 3	335±8.9	34.7±0.9	0.48±0.016	1.42
YER - 5	334±1.2	26.3±0.2	0.36±0.010	1.84
YER - 7	331±7.4	37.1±0.8	0.48±0.014	2.40
BC-412	326±2.0	51.8±1.3	0.43±0.010	1.38

It was found that in this case the attenuation characteristics are improved at the expense of the light yield readout. The main reason of this effect is, probably, due to the different solid angle selection /6/ for the two types readout systems: in the direct case the detected scintillation light solid angle is defined by the internal total reflection angle of the scintillator-air system ($\approx 42^0$), while in the FO readout case the same angle is that of the fiber-cladding system ($\approx 21^0$).

The reduced acceptance angle results in selection of light rays, in the reduced number of reflection from the surface of the scintillator and a reduced light path trough the scintillator material, and consequently in increase of the attenuation length. This is illustrated in Fig.9b. In Table 4, the attenuation characteristics of all scintillators with FO readout are shown.

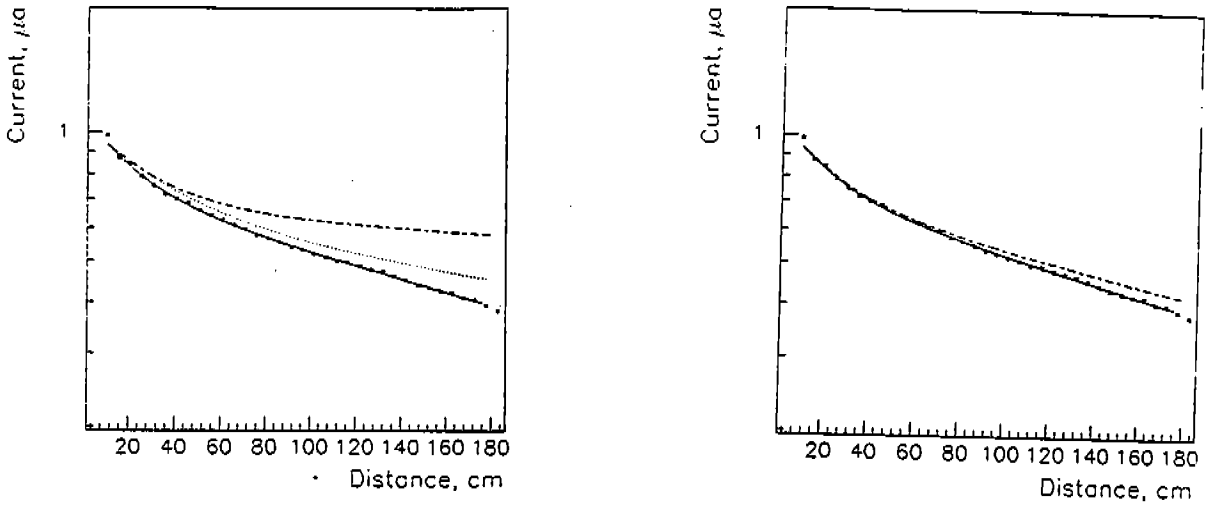

Fig.9 *Dependence of light yield from X-ray irradiation distance: a)- for "direct" readout. Points and solid curve- second side of scintillator is covered by black tape; dotted and dashed curves- same side is open and covered by aluminized mylar reflector, respectively. b)- Points and solid curves - "direct" readout, dashed curve - Fiber Optic readout. Second end of scintilletor was covered by black tape.*

The comparison of the data in the Tables 1 and 4 shows that for the Yerevan scintillators the average attenuation length with FO readout is 1.32 times more than those with direct readout. For BC-412 this ratio is 1.19 which means that the bulk attenuation length of Yerevan scintillator is longer (consequently the quality of its surface is worse).

4. Summary

We have presented here a characteristics of long scintillator strips fabricated at Yerevan Physics Institute using the extrusion method. The three main characteristics were tested: Attenuation length which have the average value of 250 cm at the direct readout and 330 cm at Fiber Optic readout; relative Light Output which is ≈45% to the anthracene and average Decay Time which is ≈2.8 nsec.. Since by the extrusion method the very long (more then 3 m) and complicated cross section scintillator strips can be fabricated our production can be used in high energy physics experiments.

Acknowledgments.

We are grateful to Ann Pla-Dalmau of the Fermilab Detector Group for measurements of the optical characteristics of SM, to Randy Wojcik for making computer software available to us, for preparing the light tight box and for some advise in methodology. We also wish to thank all staff of chemical laboratory of the Yrevan Physics Institute for scintillator material fabrication and assistance in scintillator strips extrusion.

References

[1] Bicron Handbook. Bicron corporation, 1990.
[2] NE Technology Handbook. NE Technology Ld, 1980.
[3] T.Kanon et al., NIM 213 (1983) 216.
[4] L.Nodulman et al., NIM 204 (1983) 351.
[5] V.Burkert et al., CLAS-Note-91-005, March 6, 1991.
[6] V.Burkert et al., CLAS-Note-92-008, March 31-1992.